DOI: 10.1007/s41230-016-6021-y

Microstructures and properties of rapidly solidified $Cu_{90}Zr_{10-x}Al_x$ alloys

Bing-wen Zhou [1], Xin Jiang [1], Shi-jian Yin [1], *Xing-guo Zhang [1], and Shu-ping Gou [2]

1. School of Materials Science and Engineering, Dalian University of Technology, Dalian 116024, China

2. Changchun Equipment & Technology Research Institute, Changchun 130012, China

Abstract: $Cu_{90}Zr_{10-x}Al_x$ (x=1, 3, 5, 7, 9; at.%) alloy rods were synthesized based on rapid solidification method. The structure, distribution of elements, mechanical properties and electrical conductivity of the Cu-based alloy samples were studied using X-ray diffraction (XRD), scanning electron microscope (SEM), electro-probe micro-analyzer (EPMA), uniaxial compression test and four-probe technique. The as-cast $Cu_{90}Zr_{10-x}Al_x$ (x=1, 3, 5; at.%) alloy rods with a diameter of 2 mm exhibit good mechanical properties and electrical conductivity, i.e., high compressive yield strength of 812–1513 MPa, Young's modulus of 52–85 GPa, Vickers hardness of 250–420 and electrical conductivity of 11.1%–12.6% IACS (International Annealed Copper Standard). The composite microstructure composed of high density fibrous duplex structure (Cu_5Zr and α-Cu phases) is thought to be the origin of the high strength.

Key words: copper alloys; fibrous structure; rapid solidification; mechanical properties; electrical conductivity

CLC numbers: TG146.1+1 **Document code:** A **Article ID:** 1672-6421(2016)04-262-07

Copper alloys with high strength have attracted tremendous interest for structural and functional material in high-tech fields such as microelectronics, communications, transportation and aerospace. In order to improve the strength of copper alloys, composition design and preparation technology have been widely studied [1-4]. The high strength of copper alloys has been reported to be 900 to 1,500 MPa for Cu-Be base alloys after an optimum age-hardening treatment; 600 to 1,500 MPa for Cu-M (M=Nb or Ag) alloy wires and 1,350 to 1,800 MPa for Cu-Zr alloy wires produced by the heavy cold drawing method [5-8]. To obtain the high strength performance of copper alloys, complicated subsequent manufacturing processes were needed after casting. It has been found that the highest strength of crystalline metallic material is cold-drawn Fe-C alloy (piano wire) with a fibrous structure consisting of α-Fe and Fe_3C [9, 10]. Moreover, the similar fine-structure composite with micron-sized grains in Cu-based alloys has also been proven beneficial for higher strength. For the Cu-Zr alloys, a fibrous mixed structure of α-Cu and Cu_9Zr_2 phases has been confirmed to contribute to high fracture strength [11, 12].

*** Xing-guo Zhang**

Male, born in 1960, Ph. D., Professor. His research mainly focused on the electromagnetic modification technology of light alloys, bulk metallic glasses and amorphous ribbon.

E-mail: zxgwj@dlut.edu.cn

Received: 2016-04-04; Accepted: 2016-05-01

The principles for obtaining high strength copper alloys are creating a hard second phase over the metallic matrix and using proper grain refinement technology. It is reported that a super-lattice phase of Cu_5Zr, nano-crystals of Cu_9Zr_4 and $Cu_{10}Zr_7$ have been found in $Cu_{86}Zr_{11}Al_3$ composite by copper mold casting method [13]. The super-lattice phases of Cu_5Zr separated from the matrix can effectively increase the strength. However, the electrical conductivity of $Cu_{86}Zr_{11}Al_3$ alloy is rather limited due to the distribution of nano-crystals in the copper matrix. With the aim of developing copper alloys with good mechanical properties and electrical conductivity, we present a new series of $Cu_{90}Zr_{10-x}Al_x$ (x=1–9; at.%) alloys produced by rapid solidification in this study. The microstructures and properties of Cu-Zr-Al alloys are also discussed.

1 Experimental procedure

Alloy ingots with nominal compositions of $Cu_{90}Zr_{10-x}Al_x$ (x=1,3,5,7,9; at.%) were prepared by arc melting mixtures of Cu, Zr and Al with purities of 99.99%, 99.9% and 99.99%, respectively, in a Zr-gettered high purity argon atmosphere. The ingots were melted repeatedly four times to make them chemically homogeneous. Ribbon samples with a cross section of 0.02×1.2 mm^2 were prepared by melt spinning. The injection copper mold casting method was applied to prepare alloy rods of 2 mm in diameter with 40 to 50 mm in length. The tilt casting method was

applied to prepare alloy rods of 6 mm and 20 mm in diameter with 40 to 65 mm in length. The alloy solidified in a graphite mold with a size of 30 mm×30 mm×100 mm was also prepared by the tilt casting method. The structures of the Cu-Zr-Al alloys were identified by optical microscopy (OM), X-ray diffraction (XRD) and scanning electron microscopy (SEM). The etching for OM and SEM observation specimens was made in a 0.5 pct aqueous fluoride acid solution for 5 s at 298 K (25 °C). The element distribution was analyzed using an electro-probe micro-analyzer (EPMA). Mechanical properties were measured under uniaxial compression on an Instron testing machine. In accord with ASTM standards, the samples for the compression test were prepared as 2.0 ± 0.03 mm in diameter and 4.0 ± 0.05 mm in length. Uniaxial compression tests were carried out at room temperature at a strain rate of 5×10^{-4} s^{-1}. Nano-indentation was used to measure the hardness of the phases using a Berkovitch indenter at a consistent load rate (50 $mN\cdot min^{-1}$). The fracture morphology was examined by scanning electron microscopy (SEM). Young's modulus was measured by the strain gauge. Vickers hardness was measured with a micro Vikers hardness tester (load: 25 g). Electrical conductivity measurement was made by the four-probe technique and international annealed copper standard sample with a resistivity of 1.7241 μΩcm was used as the reference material of electrical conductivity.

2 Results

Figure 1 shows the optical micrographs of the transverse cross section at the central part of the as-cast $Cu_{90}Zr_{10-x}Al_x$ (x=1–9; at.%) alloy rods with a diameter of 2 mm. The optical micrographs of $Cu_{90}Zr_9Al_1$ alloy reveal that a large number of discrete and non-directional fibrous phases separated from the supercooled liquid, which can be measured as 2–3 μm in width, 20–30 μm in length and about 30% amount in volume (Fig. 1 (a, b)). With the Zr content decreasing to 7at.% and 5at.%, the alloys solidified as a primary dendrite phase, followed by the solidification to a eutectic structure from the remaining liquid (Fig. 1c–1f). It can also be observed that the primary dendrite phase in these two alloys becomes coarse as the Zr content decreases. However, for the $Cu_{90}Zr_3Al_7$ and $Cu_{90}Zr_1Al_9$ alloys, the microstructure mainly consists of fine grains and thin grain boundaries (Fig. 1g–1j). Furthermore, in order to confirm the composition of the crystalline phases, XRD, EPMA and SEM analysis were carried out and the detailed results are shown in Figs. 2 to 5.

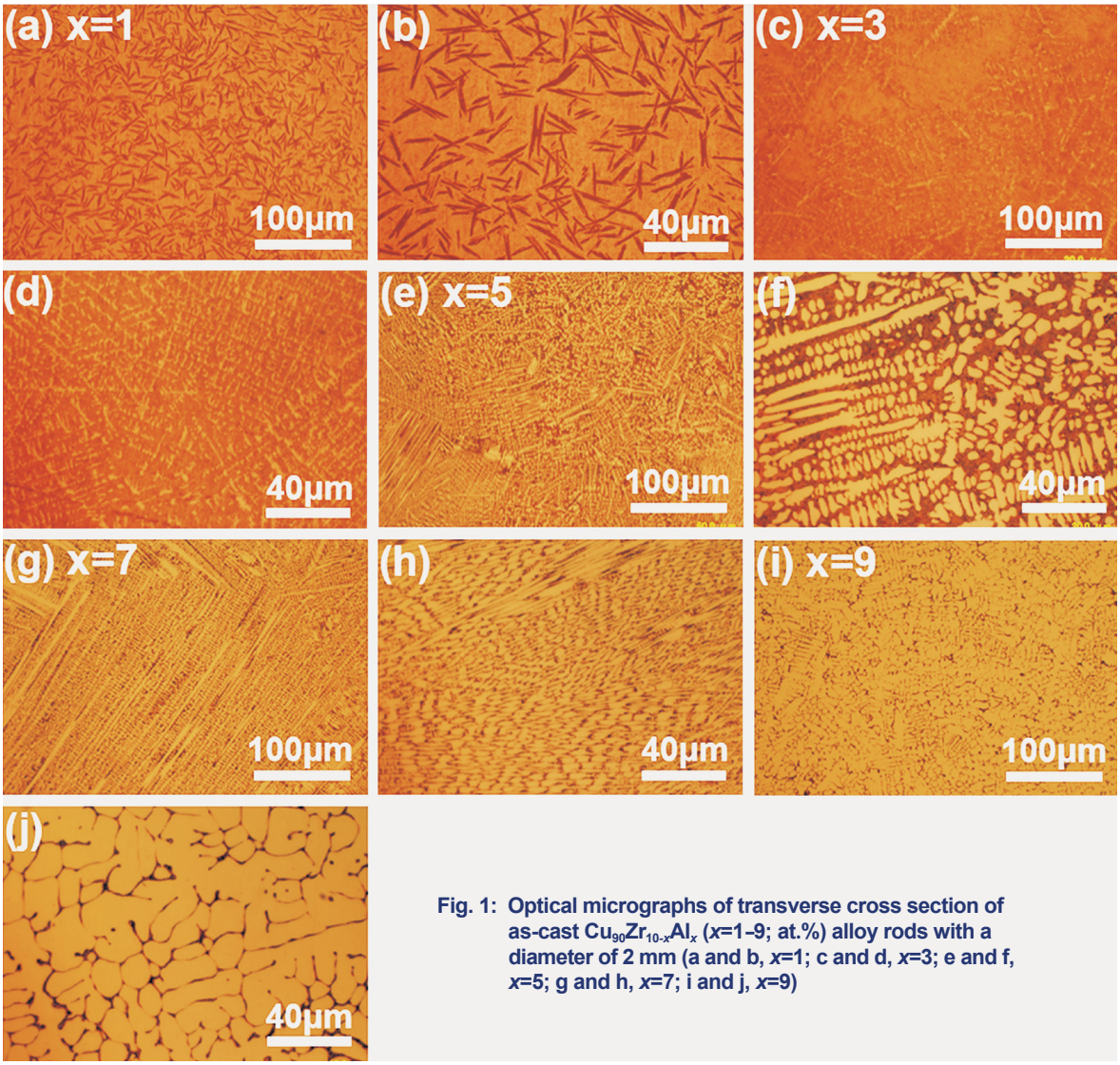

Fig. 1: Optical micrographs of transverse cross section of as-cast $Cu_{90}Zr_{10-x}Al_x$ (x=1–9; at.%) alloy rods with a diameter of 2 mm (a and b, x=1; c and d, x=3; e and f, x=5; g and h, x=7; i and j, x=9)

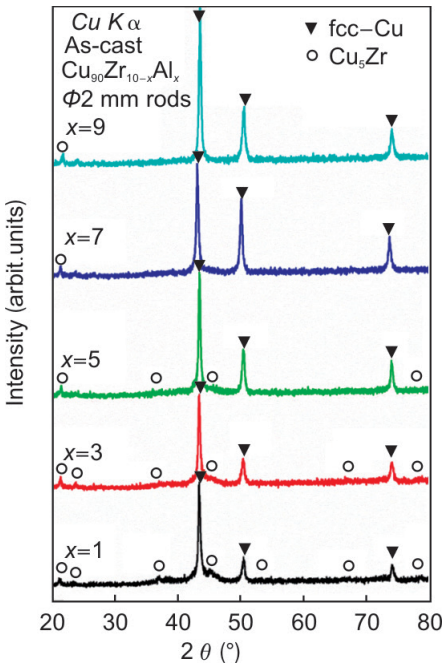

Fig. 2: XRD patterns obtained from transverse cross section of as-cast $Cu_{90}Zr_{10-x}Al_x$ (x=1, 3, 5, 7, 9; at.%) alloy rods with a diameter of 2 mm

Figure 2 shows the X-ray diffraction patterns of the as-cast $Cu_{90}Zr_{10-x}Al_x$ (x=1–9; at.%) alloy rods with a diameter of 2 mm. The X-ray diffraction patterns can be identified as two phases of α-Cu and Cu_5Zr, no other phase that contains Al can be found. It can be concluded that Al is dissolved in α-Cu and all the $Cu_{90}Zr_{10-x}Al_x$ (x=1–9; at.%) alloy rods are composed of α-Cu and Cu_5Zr phase.

Figure 3 shows the Zr distribution and Fig. 4 shows the SEM images of the transverse cross section of the as-cast $Cu_{90}Zr_{10-x}Al_x$ (x=1–9; at.%) alloy rods with a diameter of 2 mm. The Zr content in fibrous phase in $Cu_{90}Zr_9Al_1$ alloy rod is higher than that in the matrix, as shown in Fig. 3(a). Combined with the SEM image in Fig. 4(a), it can be concluded that the fibrous phase is Cu_5Zr and the matrix is a eutectic lamellar structure composed of Cu_5Zr and α-Cu. However, for the $Cu_{90}Zr_7Al_3$ and $Cu_{90}Zr_5Al_5$ alloys, the primary dendrite phase with little Zr content, as shown in Fig. 3(b, c), can be identified as α-Cu. Combined with the SEM image in Fig. 4(b, c), it can be found that the eutectic phase between the primary dendrite phases is composed of alternating layers of Cu_5Zr and α-Cu. For $Cu_{90}Zr_3Al_7$ and $Cu_{90}Zr_1Al_9$, the amount of eutectic phase decreases with a decrease in Zr content and precipitated in the α-Cu grain boundaries, as shown in Fig. 3(d, e) and Fig. 4(d, e).

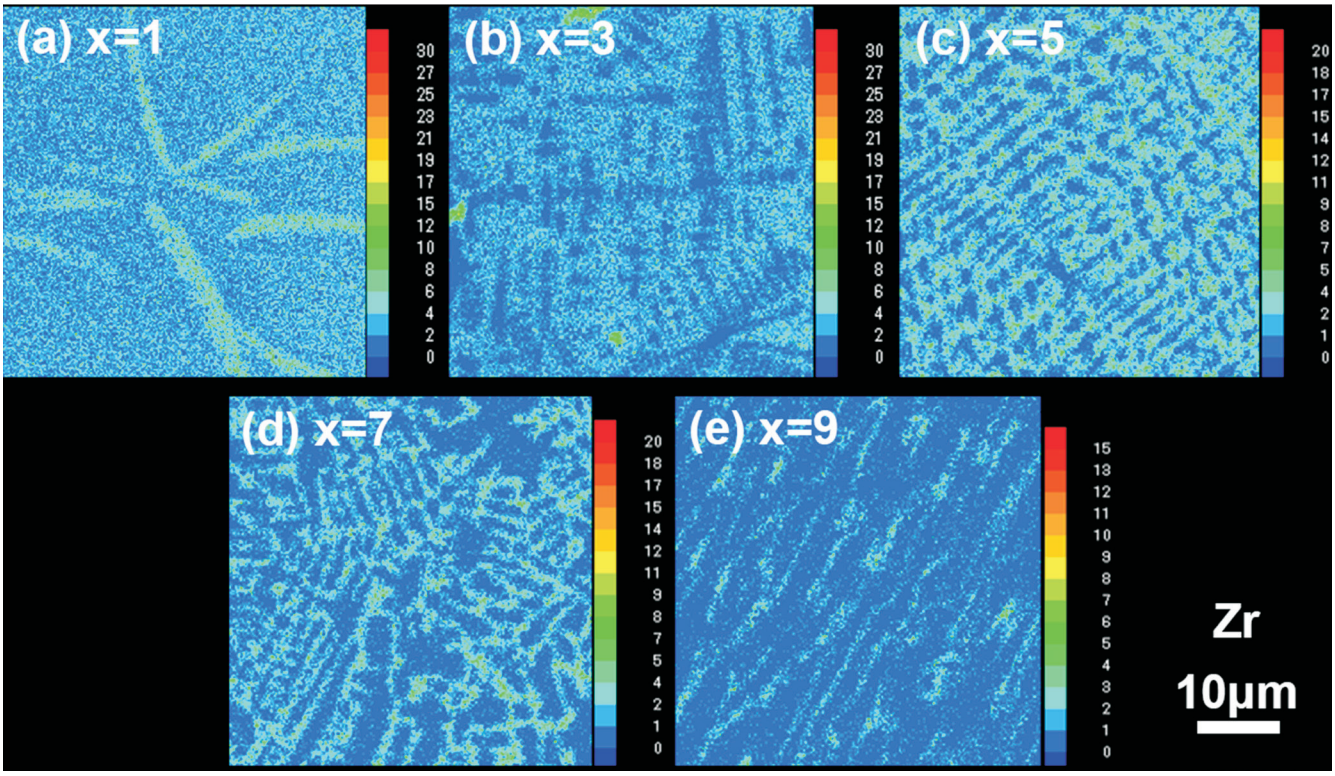

Fig. 3: Zr distribution of transverse cross section of as-cast $Cu_{90}Zr_{10-x}Al_x$ (x=1–9; at.%) alloy rods with a diameter of 2 mm (a, x=1; b, x=3; c, x=5; d, x=7; e, x=9)

In order to explore the effect of cooling rate on crystalline phases, alloy rods with a diameter of 6 mm and ribbon samples with a cross section of 0.02×1.2 mm^2 were made. Figure 5(a) shows the XRD patterns obtained from the transverse cross section of the as-cast $Cu_{90}Zr_{10-x}Al_x$ (x=1, 3, 5; at.%) alloy rods with a diameter of 6 mm. The results indicated that the similar crystalline phases can also be obtained by a lower cooling rate. However, $Cu_{90}Zr_3Al_7$ and $Cu_{90}Zr_1Al_9$ ribbon samples produced by melt spinning method with a high cooling rate are composed of a single phase α-Cu solid solution with Zr and Al, without generating other phases [Fig. 4(b, c)]. It can be concluded that high cooling rate can improve the solid solubility of the Cu alloy, but the principle components determine the crystalline phases.

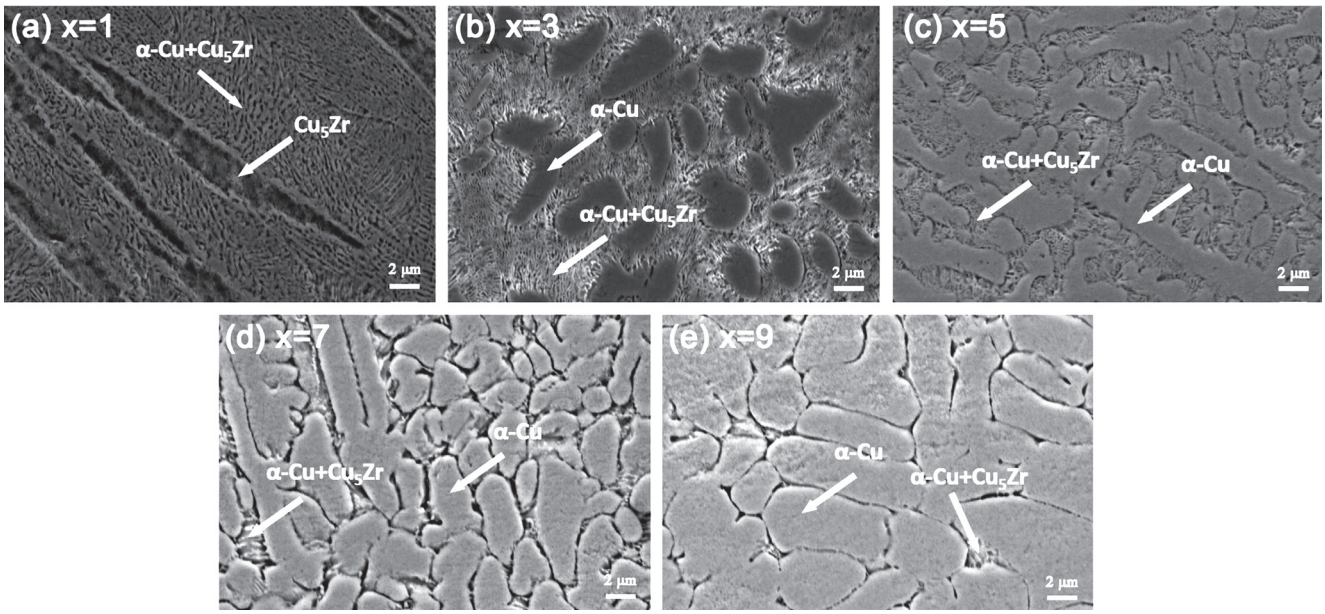

Fig. 4: SEM images of transverse cross section of as-cast $Cu_{90}Zr_{10-x}Al_x$ (x=1–9; at.%) alloy rods with a diameter of 2 mm: (a) x=1; (b) x=3; (c) x=5; (d) x=7; (e) x=9

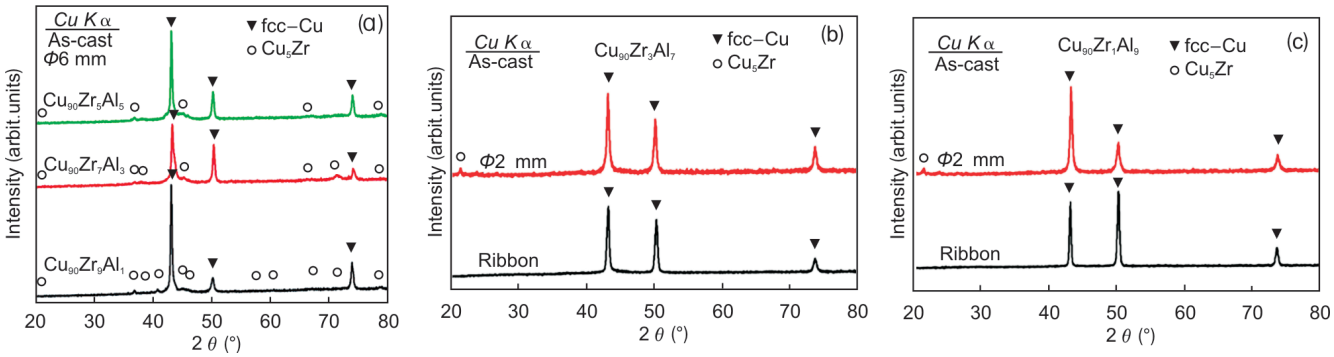

Fig. 5: XRD patterns obtained from the transverse cross section of as-cast rods and ribbon samples: (a) $Cu_{90}Zr_{10-x}Al_x$ (x=1, 3, 5; at.%); (b) $Cu_{90}Zr_3Al_7$; (c) $Cu_{90}Zr_1Al_9$

Figure 6 shows the compressive stress-strain curves of the $Cu_{90}Zr_{10-x}Al_x$ (x=1–9; at.%) as-cast alloy rods with a diameter of 2 mm. All these alloys feature large fracture strain over 50%. The $Cu_{90}Zr_9Al_1$, $Cu_{90}Zr_7Al_3$ and $Cu_{90}Zr_5Al_5$ alloys exhibit significant high compressive yield strength of 1.5, 1.0 and 0.81 GPa, respectively and high Vickers hardness of 420, 326 and 250, respectively. These unusual properties can be attributed to the fibrous Cu_5Zr phase and fine α-Cu+Cu_5Zr eutectic structure. Nano-indentation experiments were carried out to examine the roles played by the microstructures on strengthening the $Cu_{90}Zr_9Al_1$ alloy. The hardness of the primary fibrous structure and matrix structure were measured to be approximately 7.0 and 2.2 GPa, respectively. The measured hardness can then be converted to the yield strength according to equation (1) [13].

$$\Delta\sigma_\gamma\ [\mathrm{MPa}] = 274\ \Delta H_N\ [\mathrm{GPa}] \quad (1)$$

Based on this equation, the estimated yield strength of the fibrous structure and the matrix structure are approximately 1.9 and 0.6 GPa, respectively. The compressive yield strength, Young's modulus and Vickers hardness decrease with a decrease in Zr content, i.e., the depressing of Cu_5Zr phases, as shown in Table 1. Thus, it can be concluded that a well-developed fibrous

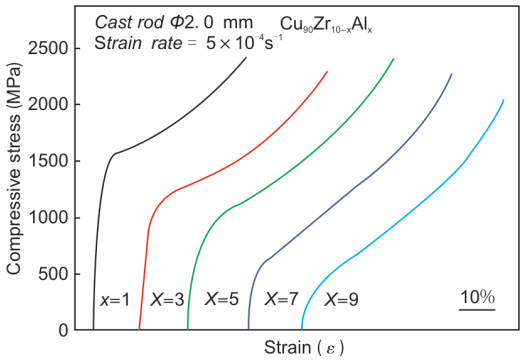

Fig. 6: Compressive stress-strain curves of the $Cu_{90}Zr_{10-x}Al_x$ (x=1, 3, 5, 7, 9; at.%) as-cast alloy rods with a diameter of 2 mm

structure with Cu_5Zr phase is thought to contribute the most to the high strength of these alloys. On the other hand, the electrical conductivity increases with a decrease in Zr content from 11.1% IACS of $Cu_{90}Zr_9Al_1$ alloy to 16.3% IACS of $Cu_{90}Zr_1Al_9$ alloy. This result indicated that the electrical conductivity remained relatively stable with the change of Zr and Al contents in these alloys. High strength Cu alloys are generally prepared by

Table 1: Average grain sizes of sand-cast and metal-cast Mg-10Gd-3Y-0.5Zr alloys

	$\sigma_{c,y}$ (MPa)	E (GPa)	Hv	%IACS
$Cu_{90}Zr_9Al_1$	1513	85	420	11.1
$Cu_{90}Zr_7Al_3$	1066	65	326	11.9
$Cu_{90}Zr_5Al_5$	812	52	250	12.6
$Cu_{90}Zr_3Al_7$	462	-	143	13.1
$Cu_{90}Zr_1Al_9$	228	-	82	16.3

complex cold working and aging process, such as commercially used electrical conductive spring material Cu-5.6at.%Ti (Cu-4.4mass%Ti), which has a tensile strength of 1,137 MPa and electrical conductivity of 10% IACS [14]. In this paper, $Cu_{90}Zr_9Al_1$ alloy rod prepared by rapid solidification exhibits a better combination of strength and electrical conductivity which may be of great potential for further application.

The SEM profiles of fractured $Cu_{90}Zr_9Al_1$ alloy samples are shown in Fig. 7. During compression, the sample's drum-like shape implies that friction occurs at the contact surfaces between the sample and the tungsten carbide platens. The friction would increase flow stress, especially in the late stage of deformation, resulting in the large increase of transversal area of the specimen and thus the decreased aspect ratio. In addition, on the outer surface of the compressive sample, the uniform flow stress has been found to change to extrusion and stack, suggesting that strain-hardening occurs by heavy deformation [15]. Hence, the increase of compressive strength after yield is the result of friction and strain-hardening.

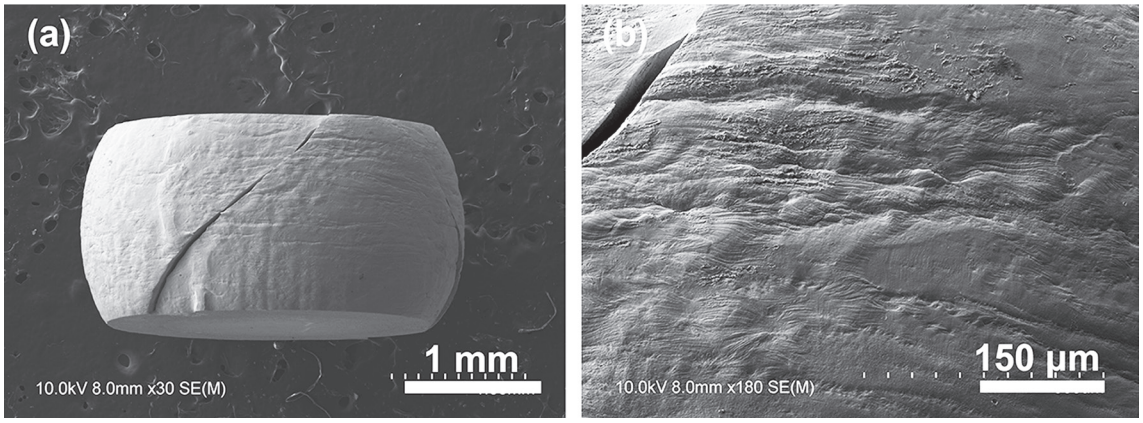

Fig. 7: SEM images of surface and fracture feature of as-cast $Cu_{90}Zr_9Al_1$ rods with a diameter of 2 mm after compressive deformation

3 Discussion

High strength Cu-Zr alloys generally have fine grains and high dislocation density through large deformation. In the present system, the addition of Zr and Al into Cu alloy (heats of mixing for Cu-Zr and Cu-Al pair are –23 kJ·mol^{-1} and –1 kJ·mol^{-1}, respectively) causes new generation of chemical affinities of Al-Zr (heats of mixing of –44 kJ·mol^{-1}) pairs, which can improve the local packing efficiency and restrain long range diffusion of atoms [16]. These factors lead to the high stability of the alloy liquid in rapid solidification process, and hence, refine the grain size of the crystallized product. Moreover, the atomic radii of the component atoms are 0.128 nm for Cu, 0.162 nm for Zr and 0.143 nm for Al, respectively [17], and hence $R_{Zr/Cu}$=1.27, $R_{Al/Cu}$=1.12 and $R_{Zr/Al}$=1.13, which is believed to introduce significant distortions of its local atomic environments due to the large atomic size mismatches and strong chemical affinities of the multi-component system.

In the rapid solidification process of copper alloy, a large degree of under-cooling and high growth rate for the initial nucleation result in deviation of the solid-liquid interface from balance [18]. The solid solubility of alloying elements in the copper matrix can be expanded and some new metastable phases can also be formed [19, 20]. The rapid solidification is considered to be a freezing mechanism formed by high solubility of Zr elements in Cu-liquid before injecting into the copper mold. On the other hand, in the $Cu_{90}Zr_{10-x}Al_x$ (x=1–9; at.%) alloys, the α-Cu phase (lattice parameters a=b=c=0.3615 nm) and the inter-metallic compound Cu_5Zr (a=b=c=0.6870 nm) have a similar orientation in the eutectic phase [11]. Thus, for the alloy containing 9at.% Zr, a small portion of Zr atoms disperse in the Cu matrix, while others may replace the Cu atoms at a substitutional or interstitial site in the α-Cu phase, resulting in the dispersive fibrous Cu_5Zr phase. With the fluctuations in the concentrations, Zr atoms almost distribute in the Cu matrix, leading to an inter-metallic compound of α-Cu+Cu_5Zr eutectic matrix structure.

It has been found that the Cu_5Zr phase exhibits high yield strength of ~1.9 GPa and high Vickers hardness of 585 [21]. In this work, it has been shown that two forms of Zr element exist in the Cu-Zr-Al alloys: the fibrous structure and eutectic structure. Whichever, the morphology and contents of Cu_5Zr phases play a significant role for high strength in this alloy series. It should be noted that the structure consisting of Cu_5Zr phases with high aspect ratio is the origin for the achievement of high strength, especially for the high yield strength above 1.5 GPa obtained for $Cu_{90}Zr_9Al_1$ alloy with fibrous duplex structure. Besides, the Cu-Zr-Al alloys with high density fibrous structure also exhibit good plasticity. It can be explained by the different deformation behavior of α-Cu and Cu_5Zr phases. After yielding, the considerable amount of α-Cu phases would enable the atoms to rearrange themselves easily to accommodate applied shear strain to high yield strength phases (Cu_5Zr) without a drastic disturbance in bonding configurations, which can account for the improved plasticity. In other words, the mismatched deformation of different phases can result in increasing the path of shear band extension and as a consequence, the plasticity of the alloys is enhanced.

In order to discuss the effects of high solidification rate on the microstructure and mechanical properties of the $Cu_{90}Zr_9Al_1$ alloy, specimens solidified at different rates have been made. Figure 8 shows optical micrographs of the as-cast $Cu_{90}Zr_9Al_1$ alloy solidified in different molds with different solidification rates. The fibrous Cu_5Zr phase of $Cu_{90}Zr_9Al_1$ alloy rod solidified in a copper mold with a diameter of 20 mm can be measured as 10–15 μm in width, 150–200 μm in length (Fig. 8b), larger than that of $Cu_{90}Zr_9Al_1$ alloy rod with a diameter of 2 mm, which was 2–3 μm in width, 20–30 μm in length as mentioned above. The compressive yield strength of the rod with a diameter of 20 mm is 1,049 MPa and the fracture strain is 10.3%. When solidified in a graphite mold with a relatively low cooling rate, the fibrous Cu_5Zr phase grows sharply to a width of 20–30 μm and length of 600–900 μm. The compressive yield strength and fracture strain are reduced to 880 MPa and 5.0%. It is obvious that high solidification rate is essential to the high strength and plasticity of $Cu_{90}Zr_9Al_1$ alloy rod with a diameter of 2 mm and the copper mold casting method is a prospective way to produce high performance copper alloys.

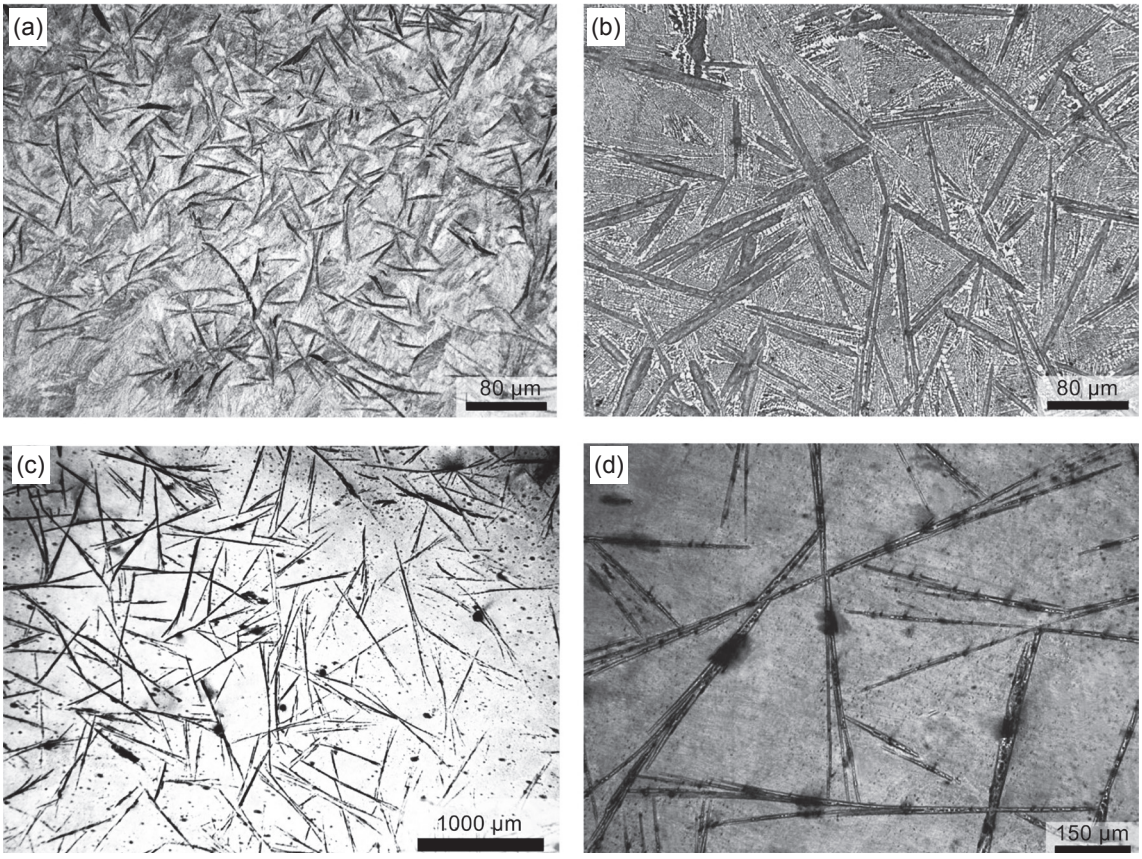

Fig. 8: Optical micrographs of as-cast $Cu_{90}Zr_9Al_1$ alloy solidified in (a) copper mold with a diameter of 2 mm; (b) copper mold with a diameter of 20 mm; (c, d) graphite mold with a size of 30×30×120 mm.

4 Conclusion

Cu-based alloys with high strength and plasticity were developed by copper mold casting, with a composite microstructure composed of high density fibrous duplex structure (α-Cu and Cu_5Zr phases). The as-cast $Cu_{90}Zr_{10-x}Al_x$ (x=1, 3, 5; at.%) alloy rods with a diameter of 2 mm exhibit good mechanical properties and electrical conductivity, i.e., high yield strength of 812-1513 MPa, Young' s modulus of 52–85 GPa, Vickers hardness of 250-420 and electrical conductivity of 11.1%–12.6% IACS. The well-developed fibrous Cu_5Zr phase with high aspect ratio and fine eutectic structure contributes to the good mechanical properties.

In addition, since the major elements of the developed alloys are Cu, Zr and Al without any toxic or costly elements, e.g., Be or Ag, and the rapid solidification method is more efficient than the traditional techniques, it can be advantageous for improving the application fields of the Cu alloys.

References

[1] Guo J Q, Yang H, Liu P, et al. Microstructure evolution and performance of Cu-10Fe-2Ag-0.15Zr in situ composite by cold rolling. Mater Res Innov, 2011, 15: 404–407.
[2] Afrasiab M, Faraji G, Tavakkoli V, et al. Excellent energy absorption capacity of nanostructured Cu-Zn thin-walled tube. Mater Sci Eng A, 2014, 599: 141–144.
[3] Zhang Xinguo, Han Jianning, Chen Liang, et al. Effects of B and Y additions on the microstructure and properties of Cu-Mg-Te alloys. J Mater Res., 2013, 28: 2747–2752.
[4] Lu Lei, Shen Yongfeng, Chen Xianhua, et al. Ultrahigh strength and high electrical conductivity in copper. Science, 2004, 304(4): 422–426.
[5] Spitzig W A, Pelton A R, and Laabs F C. Characterization of the strength and microstructure of heavily cold worked Cu-Nb composites. Acta Metallurgica, 1987, 35: 2427–2442.
[6] Sakai Y, Inoue K, Asano T, et al. Development of high-strength, high-conductivity Cu-Ag alloys for high-field pulsed magnet use. Appl Phys Lett, 1991, 59: 2965–2967.
[7] Sakai Y, and Schneider-Muntau H J. Ultra-high strength, high conductivity Cu-Ag alloy wires. Acta Mater, 1997, 45: 1017–1023.
[8] Kimura H, Inoue A, Muramatsu N, et al. Ultrahigh strength and high electrical conductivity characteristics of Cu-Zr alloy wires with nanoscale duplex fibrous structure. Mater Trans., 2006, 47: 1595–1598.
[9] Goto S, Kirchheim R, Al-Kassab T, et al. Application of cold drawn lamellar microstructure for developing ultra-high strength wires. Transactions of Nonferrous Metals Society of China, 2007, 17(6): 1129–1138.
[10] Ochiai I, Nishida S, Ohba H, et al. Application of hypereutectoid steel for development of high strength steel wire. Tetsu to Hagane, 1993, 79(9): 1101–1107.
[11] Muramatsu N, Kimura H, Inoue A. Microstructures and mechanical properties of highly electrically conductive Cu-0.5, Cu-1 and Cu-2at.%Zr alloy wires. Mater Trans., 2012, 53: 1062–1608.
[12] Muramatsu N, and Goto T. Microstructures and mechanical and electrical properties of hypoeutectic Cu-1, Cu-3 and Cu-5at.%Zr alloy wires preprocessed by spark plasma sintering. Mater Trans., 2013, 54: 1213–1219.
[13] Lee S J, Lee S W, Kim K H, et al. A high strength Cu-based alloy containing super-lattice structures. Scripta Mater., 2007, 56: 457–460.
[14] Japan Institute of Metals. Kinzoku Databook. 4th edition, Tokyo: Maruzen, 2004.
[15] Liu Y H, Wang G, Wang R J, et al. Super plastic bulk metallic glasses at room temperature. Science, 2007, 315: 1385-1388.
[16] De Boer F R, Boom R, Mattens W C M, et al. Cohesion in Metals: Transition Metal Alloys. Amsterdam: Elsevier, 1988.
[17] Japan Institute of Metals. Metals Databook. Tokyo: Maruzen, 1983.
[18] Liu F and Yang G C. Rapid solidification of highly under-cooled bulk liquid super alloy: recent developments, future directions. Inter Mater Revs, 2006, 51: 145–170.
[19] Hosseini S A and Manesh H D. High-strength, high-conductivity ultra-fine grains commercial pure copper produced by ARB processes. Mater Design, 2009, 30: 2911–2918.
[20] Glicksman M E. Principles of Solidification: An Introduction to Modern Casting and Crystal Growth Concepts. New York: Springer Science+Business Media, 2011.
[21] Kim K H, Ahn J P, Kim Y M, et al. Structural characterization and stress-relaxation behavior of super-lattice Cu_5Zr. Scripta Mater., 2008, 58: 5–8.

This study was financially supported by the National Natural Science Foundation of China (Nos. 51301029 and 51375071) and the Fundamental Research Funds for the Central Universities, China (No. DUT11RC(3)86).